Modeling, Test Benches and Identification of a Quadcopter*

João Gutemberg B. Farias Filho[1], Carlos E. T. Dórea[1],
Wallace M. Bessa[2] and João Lucas C. B. Farias[2]

***Abstract*— The mathematical modeling of the dynamics of a quadcopter using the Newton-Euler method is presented in this study. Kinematics and kinetics were developed using Euler's angles as parameters to describe the rotations of the rigid body, and all the referential changes referring to rotations were made using Coordinate Transformation Matrices. Two test benches are proposed. First a 3 degree of freedom test bench that frees the aircraft rotation while retaining the translation. The second is a one degree of freedom test bench which complements the first one. At last the test benches are used in order to identify the actuators parameters and the inertia moments.**

I. INTRODUCTION

Unmanned Aerial Vehicles (UAV) are still in a constant development in the military market. Some consider them as a technology that completely changed the military field [7]. Also, academic projects with military applications goals are more and more common ([4], [1]). On the other hand, due to cost-cutting, new civilian applications for this technology are created each day. A recent study [6] shows applications in forests and agriculture, autonomous monitoring, traffic and monitoring control, inspection systems, 3D mapping among others. These crafts can go to places of difficult access and that may be risky to humans, like the use in the Antarctic [3].

Considering the current conjuncture, this article has the following goals: establish a mathematical model of the dynamics of a quadcopter, propose two test benches which are affordable, useful and easy to build and use them to identify the model parameters of a real quadcopter.

The developed model uses the same approach as [8] and [9]. In the sense that it uses Euler's angles not quaternions [10], and uses the Newton-Euler method described in [5]. However it is a less complex model, as the motor and propeller dynamics are not being considered. Nevertheless, it is a more complete model than [11], because the assumption of small angles was not made.

The system parameters can be identified in three ways. It can be calculated using first principles models as in [12] where well stablished equations are used to find the parameters values. Also [10] uses a CAD system to generate the inertia tensor. It can be measured and updated in real time, as in [13] using adaptive control. Or it can be found through off line data analysis. This can be done by various methods, e.g. Principle of Maximum Likelihood [14], Unscented Kalman Filter [15], Prediction Error Method [16], Genetic Algorithm [17]. The approach used in this work is the third one, the parameters will be measured using the off line data. The method applied is Least Squares (LS), as in [10], the difference is that, apart from a scale, the only experimental apparatus needed are the test benches.

*This work was supported by Coordination for the Improvement of Higher Education Personnel (CAPES)

[1] João Gutemberg B. Farias Filho and Carlos E. T. Dórea are with Department of Computing Engineering and Automation, Federal University of Rio Grande do Norte, Natal-RN, Brazil.

[2] Wallace M. Bessa and João Lucas C. B. Farias are with Department of Mechanical Engineering, Federal University of Rio Grande do Norte, Natal-RN, Brazil.

II. KINEMATIC ANALYSIS OF A QUADCOPTER

At this analysis 5 points are important, the center of mass of the system (G) and the four edges of the quadcopter (A, B, C and D) where the motors and propellers are located. Fig. 1 shows the 5 points. Initially the following position vectors are known:

$$ {}_I\vec{r}_{OG} = \begin{bmatrix} x & y & z \end{bmatrix}^T \tag{1a} $$

$$ {}_{B4}\vec{r}_{GA} = \begin{bmatrix} 0 & R & 0 \end{bmatrix}^T \quad {}_{B4}\vec{r}_{GC} = \begin{bmatrix} 0 & -R & 0 \end{bmatrix}^T \tag{1b} $$

$$ {}_{B4}\vec{r}_{GB} = \begin{bmatrix} R & 0 & 0 \end{bmatrix}^T \quad {}_{B4}\vec{r}_{GD} = \begin{bmatrix} -R & 0 & 0 \end{bmatrix}^T \tag{1c} $$

where x, y and z are the components of the position vector of G relative to the origin and R is the measure of half of the quadcopter wingspan. It can be noticed by the notation of the vectors, that the first vector was expressed in the inertial frame, while the others were expressed in the frame B4, which is the fourth moving frame. Fig. 1 also illustrates this two frames of reference. In the inertial frame, the Z axis has the same direction but opposite sense of the gravitational acceleration vector, the X and Y axes can be chosen arbitrary. At the last rotational frame (B4) the frame origin is at point G, the Y axis is aligned and pointing towards point A, the X axis is also aligned and pointing towards point B.

Euler angles were used for the modeling of the quadcopter rotations, more precisely the Aeroespacial Sequence [2], which consists of a first rotation (γ) around the Z axis, a second rotation (β) around the new Y axis and a last rotation (α) around the newer X axis. These rotations are known respectively as yaw, roll and pitch.

A. Moving Frames of Reference

Four moving frames were used:

- Frame B1: represents a translational movement relative to the inertial frame, then it retains the same axes orientation. The rotation matrix is the identity matrix, ${}_{B1}\vec{r} = {}_I\vec{r}$;
- Frame B2: holds a rotation around the Z axis of frame B1, the rotation matrix is shown below.

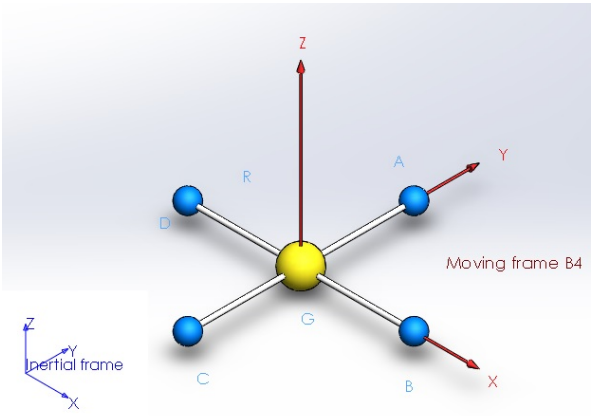

Fig. 1. Schematic model of the quadcopter showing the inertial and the B4 frames of reference.

$$ {}_{B2}\vec{r} = T_z \cdot {}_{B1}\vec{r};\ T_z = \begin{bmatrix} cos(\gamma) & sen(\gamma) & 0 \\ -sen(\gamma) & cos(\gamma) & 0 \\ 0 & 0 & 1 \end{bmatrix} \tag{2} $$

- Frame B3: holds a rotation around the Y axis of frame B2, the rotation matrix is shown below.

$$ {}_{B3}\vec{r} = T_y \cdot {}_{B2}\vec{r};\ T_y = \begin{bmatrix} cos(\beta) & 0 & -sen(\beta) \\ 0 & 1 & 0 \\ sen(\beta) & 0 & cos(\beta) \end{bmatrix} \tag{3} $$

- Frame B4: holds a rotation around the X axis of frame B3, the rotation matrix is shown below.

$$ {}_{B4}\vec{r} = T_x \cdot {}_{B3}\vec{r};\ T_x = \begin{bmatrix} 1 & 0 & 0 \\ 0 & cos(\alpha) & sen(\alpha) \\ 0 & -sen(\alpha) & cos(\alpha) \end{bmatrix} \tag{4} $$

As the matrices T_x, T_y and T_z are orthogonal, the equality $T_x^{-1} = T_x^T$ is true.

B. Rotation Vectors

1) Angular velocity vectors for individual rotations: these vectors stand for each single rotation the quadcopter does, i.e., yaw, roll and pitch.

$$ {}_I\dot{\gamma} = {}_{B1}\dot{\gamma} = \begin{bmatrix} 0 \\ 0 \\ \dot{\gamma} \end{bmatrix},\ {}_{B2}\dot{\beta} = \begin{bmatrix} 0 \\ \dot{\beta} \\ 0 \end{bmatrix}\ e\ {}_{B3}\dot{\alpha} = \begin{bmatrix} \dot{\alpha} \\ 0 \\ 0 \end{bmatrix} \tag{5} $$

2) Body's angular velocity and angular acceleration vectors: these represent all of the body individual rotations combined.

$$ {}_I\vec{\omega} = {}_I\dot{\gamma} + T_z^T\, {}_{B2}\dot{\beta} + T_z^T\, T_y^T\, {}_{B3}\dot{\alpha} \quad {}_{B4}\vec{\omega} = T_x\ T_y\ T_z\ {}_I\vec{\omega} \tag{6a} $$

$$ {}_I\dot{\vec{\omega}} = \frac{d}{dt}({}_I\vec{\omega}) \quad {}_{B4}\dot{\vec{\omega}} = T_x\ T_y\ T_z\ {}_I\dot{\vec{\omega}} \tag{6b} $$

C. Kinematics of the center of mass (G)

The center of mass does not carry any rotational effect, this point describes all the translational kinematics of the quadcopter.

$$ {}_I\vec{r}_{OG} = \begin{bmatrix} x \\ y \\ z \end{bmatrix},\ {}_I\vec{v}_G = \begin{bmatrix} \dot{x} \\ \dot{y} \\ \dot{z} \end{bmatrix}\ e\ {}_I\vec{a}_G = \begin{bmatrix} \ddot{x} \\ \ddot{y} \\ \ddot{z} \end{bmatrix} \tag{7} $$

D. Kinematics of the points A, B, C and D

The position vector only is expanded. The velocity and acceleration vectors are shown in them literal form.

- Point A:

$$ {}_I\vec{r}_{OA} = {}_I\vec{r}_{OG} + {}_I\vec{r}_{GA} = {}_I\vec{r}_{OG} + T_z^T T_y^T T_x^T\, {}_{B4}\vec{r}_{GA} \tag{8a} $$

$$ {}_I\vec{r}_{OA} = \begin{bmatrix} (\cos(\gamma)\sin(\alpha)\sin(\beta) - \sin(\gamma)\cos(\alpha))\, R + \mathrm{x} \\ (\sin(\gamma)\sin(\alpha)\sin(\beta) + \cos(\gamma)\cos(\alpha))\, R + \mathrm{y} \\ \sin(\alpha)\cos(\beta)\, R + \mathrm{z} \end{bmatrix} \tag{8b} $$

$$ {}_I\vec{v}_A = {}_I\vec{v}_G + {}_I\vec{\omega} \times {}_I\vec{r}_{GA} \tag{8c} $$

$$ {}_I\vec{a}_A = {}_I\vec{a}_G + {}_I\dot{\vec{w}} \times {}_I\vec{r}_{GA} + {}_I\vec{w} \times ({}_I\vec{w} \times {}_I\vec{r}_{GA}) \tag{8d} $$

The kinematics of points B, C and D can be found analogously.

III. KINETIC ANALYSIS OF A QUADCOPTER

A. Inertia Tensor

Under the assumption that the system is symmetrical in all three axes, the inertia tensor will only have non-zero components in the main diagonal, as shown bellow.

$$ {}_{B4}\bar{\bar{I}}_G = \begin{bmatrix} I_{xx} & 0 & 0 \\ 0 & I_{yy} & 0 \\ 0 & 0 & I_{zz} \end{bmatrix} \tag{9} $$

where I_{xx}, I_{yy} and I_{zz} are the main components of the inertia tensor for the X, Y and Z axes.

B. External forces and Newton's Second Law

The thrust produced by the propellers appear in the model as forces acting always in the direction of the motors axes and pointing from the motor to the propellers. The forces always points to the +Z axis of the frame B4. Besides the propellers thrusts, the other acting force will be the system's weight. Thus the forces are:

$$ {}_{B4}\vec{F}_A = \begin{bmatrix} 0 & 0 & F_A \end{bmatrix}^T\ {}_{B4}\vec{F}_B = \begin{bmatrix} 0 & 0 & F_B \end{bmatrix}^T \tag{10a} $$

$$ {}_{B4}\vec{F}_C = \begin{bmatrix} 0 & 0 & F_C \end{bmatrix}^T\ {}_{B4}\vec{F}_D = \begin{bmatrix} 0 & 0 & F_D \end{bmatrix}^T \tag{10b} $$

$$ {}_I\vec{P} = \begin{bmatrix} 0 & 0 & -mg \end{bmatrix}^T \tag{10c} $$

where F_A is the thrust force produced by the propeller located at point A. F_B, F_C and F_D are analogous. The quadcopter mass is m, g is the gravitational acceleration and $\vec{P}$ is the weight vector.

Then, adding all forces in the inercial frame and applying Newton's Second Law:

$$ \sum {}_I\vec{F} = m \cdot {}_I\vec{a}_G \tag{11} $$

C. External Moments

1) Produced by the propellers thrust: the moments will be calculated relative to the center of mass (G). Each thrust force produces a moment which can be given by the cross product between the position vector of the force's point of application relative to the point G, and the force's vector.

$$ {}_{B4}\vec{M}_{A,G} = \begin{bmatrix} R \cdot F_A \\ 0 \\ 0 \end{bmatrix} \quad {}_{B4}\vec{M}_{B,G} = \begin{bmatrix} 0 \\ -R \cdot F_B \\ 0 \end{bmatrix} \tag{12a} $$

$$ {}_{B4}\vec{M}_{C,G} = \begin{bmatrix} -R \cdot F_C \\ 0 \\ 0 \end{bmatrix} \quad {}_{B4}\vec{M}_{D,G} = \begin{bmatrix} 0 \\ R \cdot F_D \\ 0 \end{bmatrix} \tag{12b} $$

2) Produced by the motor torque: this moment can be described as being proportional to the thrust force generated by the propeller. The proportionality constant, R_H, will be explained later in Section VII.

In a quadcopter is usual to have two motors turning clockwise (CW) and the other two turning counterclockwise (CCW). As the Z axis points up, CCW means a positive rotation and CW means a negative rotation. It shall be considered that the motors A and C will turn CW and the motors B and D will turn CCW. As the chassis reacts in the opposite direction of the motors, A and C will produce a positive moment and B and D will produce a negative moment. Therefore:

$$ {}_{B4}\vec{M}_{H,A} = \begin{bmatrix} 0 \\ 0 \\ R_H \cdot F_A \end{bmatrix} \quad {}_{B4}\vec{M}_{H,B} = \begin{bmatrix} 0 \\ 0 \\ -R_H \cdot F_B \end{bmatrix} \tag{13a} $$

$$ {}_{B4}\vec{M}_{H,C} = \begin{bmatrix} 0 \\ 0 \\ R_H \cdot F_C \end{bmatrix} \quad {}_{B4}\vec{M}_{H,D} = \begin{bmatrix} 0 \\ 0 \\ -R_H \cdot F_D \end{bmatrix} \tag{13b} $$

D. Newton's Second Law Applied to Rotation

We sum the moments, in the B4 frame of reference, then apply Newton's Second Law:

$$ \sum {}_{B4}\vec{M}_G = {}_{B4}\bar{\bar{I}}_G \, \frac{d}{dt}({}_{B4}\vec{w}) + {}_{B4}\vec{w} \times {}_{B4}\bar{\bar{I}}_G \, {}_{B4}\vec{w} \tag{14} $$

IV. MOTION EQUATIONS

After the kinematic and kinect analyses, 6 non-linear ODE's are obtained. These equations describes the system complete dynamics, both translational and rotational which allows for the simulation of the system behavior. Using c as an abbreviation of cos and s as an abbreviation of sin, the first three equations below derive from (11):

$$ (c(\gamma)\, c(\alpha)\, s(\beta) + s(\gamma)\, s(\alpha))\, (F_A + F_B + F_C + F_D) = m \cdot \ddot{x} \tag{15a} $$

$$ (s(\gamma)\, c(\alpha)\, s(\beta) - c(\gamma)\, s(\alpha))\, (F_A + F_B + F_C + F_D) = m \cdot \ddot{y} \tag{15b} $$

$$ c(\alpha)\, c(\beta)\, (F_A + F_B + F_C + F_D) - mg = m \cdot \ddot{z} \tag{15c} $$

The next three equations derive from (14):

$$ \begin{aligned} &R \cdot (F_A - F_C) = (Iyy - Izz)\, c(\alpha)\, s(\alpha)\, \dot{\beta}^2 + \\ &Ixx\, (-\dot{\gamma}\, c(\beta)\, \dot{\beta} - \ddot{\gamma}\, s(\beta) + \ddot{\alpha}) + ((2\, Iyy - 2\, Izz)\, \dot{\gamma}\, s(\alpha)^2 \\ &+ (Izz - Iyy)\, \dot{\gamma})\, c(\beta)\, \dot{\beta} + (Izz - Iyy)\, \dot{\gamma}^2\, c(\alpha)\, s(\alpha)\, c(\beta)^2 \end{aligned} \tag{16a} $$

$$ \begin{aligned} &R \cdot (F_D - F_B) = Iyy\, (c(\alpha)\, \ddot{\beta} - \dot{\gamma}\, s(\alpha)\, s(\beta)\, \dot{\beta} - s(\alpha)\, \dot{\alpha}\, \dot{\beta} + \\ &\dot{\gamma}\, c(\alpha)\, \dot{\alpha}\, c(\beta) + \ddot{\gamma}\, s(\alpha)\, c(\beta)) + ((Ixx - Izz)\, \dot{\gamma}\, s(\alpha)\, s(\beta) + \\ &(Izz - Ixx)\, s(\alpha)\, \dot{\alpha})\, \dot{\beta} + (Izz - Ixx)\, \dot{\gamma}^2\, c(\alpha)\, c(\beta)\, s(\beta) + \\ &(Ixx - Izz)\, \dot{\gamma}\, c(\alpha)\, \dot{\alpha}\, c(\beta) \end{aligned} \tag{16b} $$

$$ \begin{aligned} &R_H \cdot (F_A + F_C - F_B - F_D) = Izz\, (-s(\alpha)\, \ddot{\beta} - \\ &\dot{\gamma}\, c(\alpha)\, s(\beta)\, \dot{\beta} - c(\alpha)\, \dot{\alpha}\, \dot{\beta} - \dot{\gamma}\, s(\alpha)\, \dot{\alpha}\, c(\beta) + \ddot{\gamma}\, c(\alpha)\, c(\beta)) + \\ &((Ixx - Iyy)\, \dot{\gamma}\, c(\alpha)\, s(\beta) + (Iyy - Ixx)\, c(\alpha)\, \dot{\alpha})\, \dot{\beta} + \\ &(Ixx - Iyy)\, \dot{\gamma}^2\, s(\alpha)\, c(\beta)\, s(\beta) + (Iyy - Ixx)\, \dot{\gamma}\, s(\alpha)\, \dot{\alpha}\, c(\beta) \end{aligned} \tag{16c} $$

V. QUADCOPTER

The quadcopter (Fig. 2) used in this study is not a commercial model as it was built using the following parts:

- Intel Edison and its arduino breakout board as the flight controller;
- The GY-87 sensor board, which has a 3 axes accelerometer, a 3 axes gyroscope, a 3 axes magnetometer and a barometer;
- Four HobbyKing BlueSeries 30 A electronic speed controllers;
- Four Turnigy D2830-11 1000 kv brushless motors;
- Four 10 inch diameter 4.5 inch pitch propellers (2 CW and 2 CCW);
- ZIPPY Flightmax 5000 mAh 3S1P 20C battery;
- Hobbyking SK450 45 cm fiber glass frame.

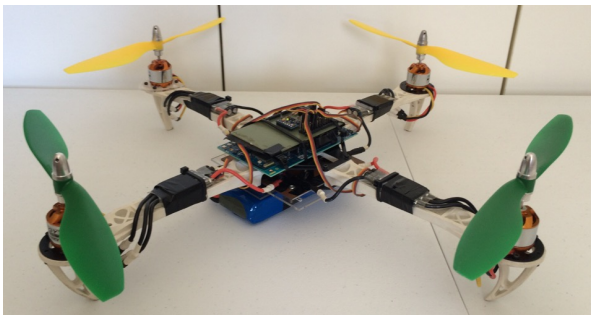

Fig. 2. Quadcopter used in this study.

The system has $1.20\ kg$ of mass and a wingspan of $0.45\ m$.

VI. TEST BENCHES

The model developed in the previous sections can be used for simulations of the system behavior and control design. However, some model parameters must be estimated in order to make it reproduce the system behavior as close as possible. A test bench ensure all the tests can be made in a secure and controlled way. Besides that, it can be a very useful instrument to help in the identification of the parameters, as will be shown in Section VII.

A. First test bench

The first test bench was built in such a way that it allows the quadcopter to change its orientation in three degrees of freedom, but keeping its position fixed. The craft is completely free to rotate but cannot translate.

The bench consists of a support and a rotation joint. The support is shaped as a pedestal with a housing and bearing to receive a vertical axis in its top.

The rotation joint that was chosen is based on a cardan joint (also known as universal joint), Fig. 3, commonly used to transmit power between angled axes. The joint itself allows the two pieces it connects to move, one relative to the other, around two distinct rotation axes (perpendicular to the longitudinal axis of the joint itself). The support will be located on one side of the joint and the quadcopter on the other side.

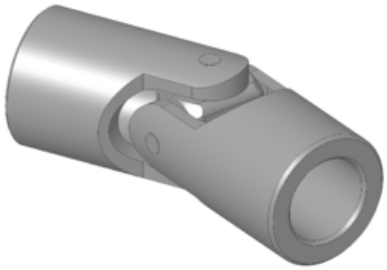

Fig. 3. Cardan Joint (wikipedia.com)

Once the cardan joint is connected to the housing and bearing in the support, this coupling allows the joint to rotate freely in its longitudinal axis. At last, the quadcopter will be able to rotate, relative to the support, in three perpendicular axes, two of them due to the cardan joint and one due to the coupling between the joint and the support.

The coupling between the joint and the quadcopter is rigid. A thin plate can be welded to the joint and the plate itself screwed to the quadcopter, for example.

Fig. 4. First test bench mounted.

The test bench enforces the system to rotate around the cardan axes. When those axes do not match the quadcopter center of mass, the system own weight exercise a moment that adds up to a pendular behavior. For this reason, the bench shall be mounted in a way that minimizes the distance between the cardan joint center of rotation and the system center of mass.

It is easy to align the x and y components of the cardan rotation center with the quadcopter center of mass. But it is not always possible to align the z component, as generally there is not much space left in the center of the quadcopter due to the electronics, cables and battery.

This z component difference can result in a considerable increase of the measured inertia moments I_{xx} and I_{yy}. The inertia moment I_{zz} remains unchanged. To circumvent this problem, a second test bench was created.

B. Second test bench

As it is not always possible to align the cardan rotation center to the system rotation center, this second test bench was developed and, although simpler, complements the previous one.

The test bench consists of two supports, each acting as a bearing to a shaft. If one drills the quadcopter's landing feet to match the shafts diameter, it is possible to mount two opposite feet to the supports. This allows the system to rotate around one axis at a time, the pitch or the roll axis. Fig. 5 shows in detail the supports, the shafts, and the drilled feet.

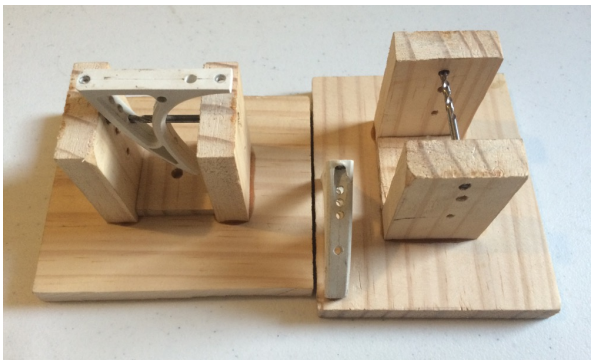

Fig. 5. Second test bench. Detail of the supports, shafts and quadcopter's drilled feet.

By making several holes in the feet at different heights it is possible to find the approximate height which matches the quadcopter center of rotation.

This bench allows a greater precision in the identification of the inertia moments I_{xx} and I_{yy}. It can also be used to test and design the controller around the α and β angles. Fig. 6 shows the system mounted on the test bench.

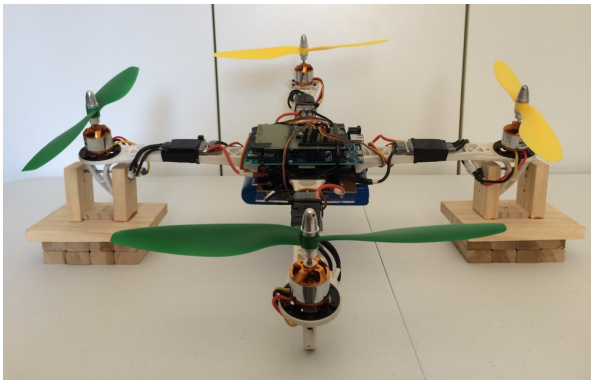

Fig. 6. System mounted in the second test bench.

VII. IDENTIFYING THE MODEL PARAMETERS

A. Parameters of the actuators

1) Thrust parameters (k_{Ha}, k_{Hb}): the thrust a propeller generates can be modeled as ([10], [18]):

$$F = k_T \, \omega_H^2 \tag{17}$$

where k_T is the propeller thrust constant and ω_H is the propeller angular velocity.

Generally, the motor speed is controlled by a PWM signal, measured by its pulse width (T_{pw}) in microseconds. According to [8], the propeller thrust is also approximately linearly proportional to the PWM signal. Therefore,

$$F = k_{Ha} \, T_{pw} + k_{Hb} \tag{18}$$

where k_{Ha} and k_{Hb} are the parameters of the straight line equation.

By using one of the test benches it is possible to control one motor and place the opposite edge over a scale, so one can measure the thrust generated by the controlled motor. The obtained data from all the motors are depicted in Fig. 7, from which its possible to find, through LS, the values $k_{Ha} = 0.0099 \; N/\mu s$ and $k_{Hb} = -10.8766 \; N$.

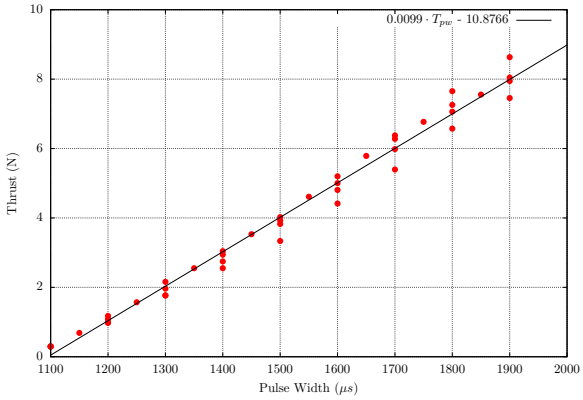

Fig. 7. Pulse width in μs versus propeller thrust in N.

2) Torque parameter (R_H): the equation below shows how to calculate the torque produced by the motor (τ_M) ([10], [18])

$$\tau_M \approx k_D \, \omega_H^2 \tag{19}$$

where k_D is the drag coefficient.

Next, combining (17) and (19),

$$\tau_M \approx \frac{k_D}{k_T} \, F = R_H \, F \tag{20}$$

where R_H is the proportionality constant between the propeller thrust and the motor torque.

To find experimentally the torque produced by the motor and hence the parameter R_H, one can use the first test bench and control two opposite motors. By maintaining the two motors with the same angular velocity and controlling this velocity, the resultant moment in the test bench will act only in the Z axis. So it is possible to connect one of the quadcopter edges to a dynamometer (or use again a scale) and measure the produced force. This force can be multiplied by the half wingspan R to find the moment. The moment value should be divided by two, so that only one motor contribution is accounted. After that it is possible to trace a curve of torque by thrust and use LS to find R_H. Fig. 8 shows the obtained torque versus thrust data, for all motors, resulting in $R_H = 0.0185 \; m$.

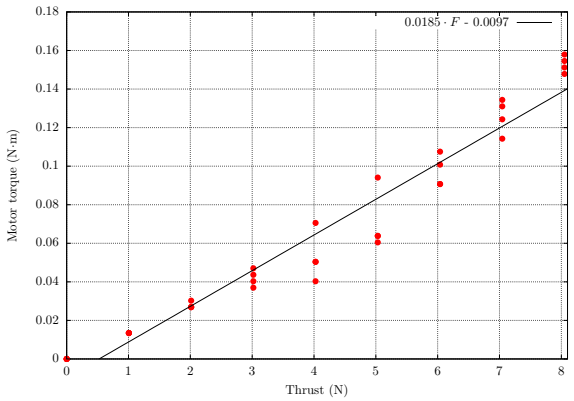

Fig. 8. Motor torque in $N \cdot m$ versus propeller thrust in N.

B. Inertia Tensor

In order to calculate the moments of inertia in each axis X, Y and Z a known and constant force is needed. The force can be caused by the system itself (motor actuation) if the parameters were already computed, or a known mass can be used to generate a moment. The actuation on the axes is done one at a time, that is, in order to find I_{xx}, we set $\beta = \dot{\beta} = \ddot{\beta} = 0$ and $\gamma = \dot{\gamma} = \ddot{\gamma} = 0$ and the angle is actuated only in α. This way, the movement equation (16a) reduces to:

$$I_{xx} = \frac{R \cdot (F_A - F_C)}{\ddot{\alpha}} \quad \text{or} \quad I_{xx} = \frac{M_{ext}}{\ddot{\alpha}} \tag{21}$$

where M_{ext} would be an external moment applied to the system. Analogously, for I_{yy} and I_{zz}:

$$I_{yy} = \frac{R \cdot (F_D - F_B)}{\ddot{\beta}} \quad \text{or} \quad I_{yy} = \frac{M_{ext}}{\ddot{\beta}} \tag{22}$$

$$I_{zz} = \frac{R_H \cdot (F_A + F_C - F_B - F_D)}{\ddot{\gamma}} \quad \text{or} \quad I_{zz} = \frac{M_{ext}}{\ddot{\gamma}} \tag{23}$$

After applying the force, the data recorded by the sensors of the quadcopter can be used to graph α by time. With a constant force, the generated acceleration is constant too. A constant acceleration generates a parabola as a graph and its quadratic coefficient is $\ddot{\alpha}/2$. Finding $\ddot{\alpha}$, gives I_{xx}. It is also possible to graph $\dot{\alpha}$ versus time and look for a section of the graph in which the curve behaves like a straight line, meaning that the acceleration is constant in the section. The line coefficient of the straight line is $\ddot{\alpha}$. The same applies for β and γ.

the second test bench was used to find I_{xx} and I_{yy}. An external moment was applied by using a known mass object at a known distance of the rotation center. The resulting moment was $M_{ext} = 0.125 \; N \cdot m$. Fig. 9 and Fig. 10 shows the behavior of α and β. The computed values were $I_{xx} = 0.015 \; kg \cdot m^2$ and $I_{yy} = 0.015 \; kg \cdot m^2$.

The first test bench was used to find I_{zz} and the torque was generated by applying a 1300 pulse width signal to each one

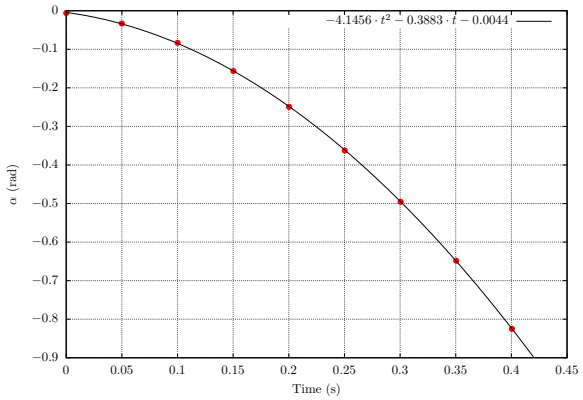

Fig. 9. Behavior of α caused by a constant moment.

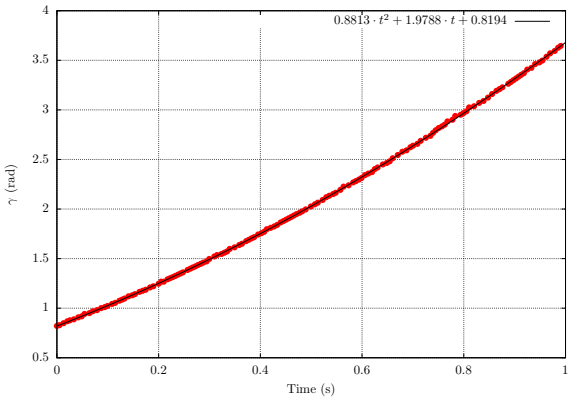

Fig. 11. Behavior of γ caused by a constant moment.

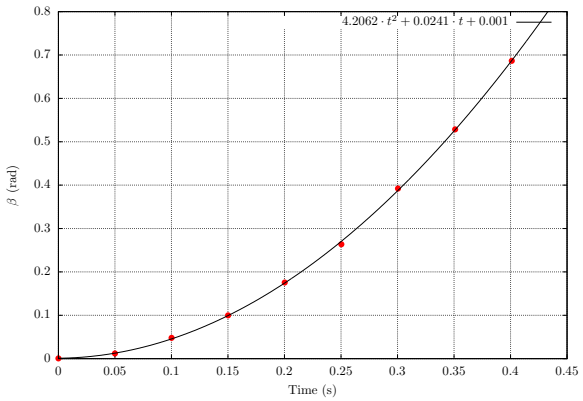

Fig. 10. Behavior of β caused by a constant moment.

of two opposite motors. The resulting torque was $0.055\ N{\cdot}m$. Fig. 11 shows the behavior of γ. The computed value was $I_{zz} = 0.031\ kg \cdot m^2$.

VIII. CONCLUSION

For a satisfactory control performance, especially in model based control, one needs a reliable model which reproduces as close as possible the behavior of the real system to be controlled. This work aimed in providing the base for a subsequent control of a quadcopter by developing a model, proposing the test benches and using them to identify the model parameters.

The test benches were useful to find all the needed model parameters but they can also be used to test the control strategy (for attitude) in a secure way for both the designer and the system itself.

REFERENCES

[1] Ganglin, W., Key parameters and conceptual configuration of unmanned combat aerial vehicle concept, Chinese Journal of Aeronautics, Vol. 22, pp. 393–400, 2009.

[2] Kuipers, J.B., Quaternions and Rotation Sequences, Princeton University Press, Princeton, USA, pp. 400, 2002.

[3] Lucieer, A., Turnera, D., King, D.H. e Robinson, S.A., Using an unmanned aerial vehicle (uav) to capture micro- topography of antarctic moss beds, International Journal of Applied Earth Observation and Geoinformation, Vol. 27, pp. 53–62, 2014.

[4] Nguyen, N.V., Choi, S.M., Kim, W.S., Lee, J.W., Kim, S., Neufeld, D. e Byun, Y.H., Multidisciplinary unmanned combat air vehicle system design using multi-fidelity model, Aerospace Science and Technology, Vol. 26, pp. 200- 210, 2013.

[5] Santos, I.F., Dinâmica de Sistemas Mecânicos, Makron Books, São Paulo, Brasil, pp. 272, 2001.

[6] Siebert, S. e Teizer, J., Mobile 3d mapping for surveying earthwork projects using an unmanned aerial vehicle (uav) system, Automation in Construction, Vol. 41, pp. 1–14, 2014.

[7] Stulberg, A.N., Managing the unmanned revolution in the u.s. air force, Orbis, Vol. 51, pp. 251–265, 2007.

[8] Zhang, D., Qi, H., Wu, X., Xie, Y. and Xu, J., The Quadrotor Dynamic Modeling and Indoor Target Tracking Control Method, Mathematical Problems in Engineering, Vol. 2014, 9p, 2014.

[9] Gharib, M. R. and Moavenian, M., Full dynamics and control of a quadrotor using quantitative feedback theory, International Journal of Numerical Modelling: Electronic Networks, Devices and Fields, Vol. 29, pp. 501-519, 2015.

[10] Chovancova, A., Fico, T., Chovanec, L. and Hubinsky, P., Mathematical Modelling and Parameter Identification of Quadrotor (a survey), Modelling of Mechanical and Mechatronic Systems, Vol. 96, pp. 172-181, 2014.

[11] Santana, P.H.R.Q.A. and Borges, G.A., Modelagem e controle de quadrirrotores, In IX Simpósio Brasileiro de Automação Inteligente (SBAI 2009), Vol. 9, pp. 1-6, 2009.

[12] Bresciani, T., Modelling, Identification and Control of a Quadrotor Helicopter, MSc Thesis, Department of Automatic Control Lund University, 2008.

[13] Lopéz, R., Gonzalez, I., Flores, J., Ordaz, J., Salazar, S. and Lozano, R., Real Time Parameter Identification of the Inertia Tensor for a Quad-rotor mini-aircraft using Adaptive Control, 2nd IFAC Workshop on Research, Education and Development of Unmanned Aerial Systems, vol. 2, pp. 6 2013.

[14] Bottasso, C.L., Leonello, D., Maffezzoli, A. and Riccardi, F., A procedure for the identification of the inertial properties of small-size RUAVs, 35th European Rotorcraft Forum, 2009.

[15] Abas, N., Legowo, A. and Akmeliawati, R., Parameter Identification of an Autonomous Quadrotor, 2011 4th International Conference on Mechatronics, 2011.

[16] Schreurs, R. J. A., Weiland, S., Zhang, H. T. Q., Zhu, Y., and Xu, C., Open Loop System Identification of a Quadrotor Helicopter System, 10th IEEE International Conference on Control and Automation, pp. 1702-1707, 2013.

[17] Yang, J., Cai, Z., Lin, Q., Zhang, D. and Wang, Y., System Identification of Quadrotor UAV Based on Genetic Algorithm, Proceedings of 2014 IEEE Chinese Guidance, Navigation and Control Conference, 2014.

[18] Rinaldi, F., Chiesa, S. and Quagliotti, F., Linear Quadratic Control for Quadrotors UAVs Dynamics and Formation Flight, Journal of Intelligent & Robotic Systems, vol. 70, pp. 203-220, 2012.